Caving 2026 – A van As, D Cumming-Potvin & J Wesseloo (eds)

doi:10.36487/ACG_repo/2645_06

Geotechnical basis of design and early cave performance at Hugo North Lift 1, Oyu Tolgoi

Lawrence Rwodzi [a,*], Josef Ekkerd [b], Karta Simanjuntak [b], Baatarzorigt Baasanjav [a], Johnson Ooi [a]

[a] *Oyu Tolgoi, Rio Tinto, Mongolia*

[b] *Oyu Tolgoi, Rio Tinto, Australia*

Abstract

The Hugo North Lift 1 (HNL1) block cave at Oyu Tolgoi is a large-footprint, deep (~1,300 m) cave developed in a structurally complex porphyry copper–gold system under high in situ stress conditions ($\sigma_1 \approx 57.8$ MPa) and fair-to-poor rock mass quality. Panel 0, the first of four planned mining blocks, was undercut between 2022 and 2024 and has successfully propagated to surface, providing a unique performance dataset for block caving at this depth and stress regime.

This paper documents the geotechnical basis of design (BoD) for HNL1, including the design evolution from feasibility through execution and key refinements to footprint geometry, advanced undercutting methodology, cave initiation criteria and macroblock sequencing. Panel 0 performance is then assessed against BoD predictions, with observed outcomes used to validate design assumptions and extract key learnings.

Results demonstrate alignment between predicted and observed cave behaviour, including undercut advance rates, cave initiation hydraulic radius, infrastructure performance and successful full-height cave propagation. The combined BoD and performance record establishes a benchmark technical reference for the design and operation of deep, high-stress porphyry block caves and provides guidance for reducing geotechnical uncertainty in future large-scale cave mining projects.

Keywords: *Oyu Tolgoi, block cave, geotechnical basis of design, footprint geometry, deep high-stress, complex geology*

1 Introduction

Hugo North Lift 1 (HNL1) is among the world's deepest block caves, with an extraction level located approximately 1,300 m below surface. The cave is developed within a structurally complex porphyry copper–gold deposit and is characterised by high in situ stress and moderate-to-poor rock mass quality. The mine design comprises approximately 215 km of lateral development, five shafts and 1,488 drawpoints distributed across four planned mining blocks. Figure 1 provides a layout of HNL1 mining blocks and access infrastructure.

Industry benchmarking by Mawdesley & Altankhuu (2026) as shown in Figure 2, places HNL1 alongside the Deep Mill Level Zone, Grasberg Block Cave, Cadia East, Chuquicamata and Henderson as one of the deepest active or recently commissioned block caves globally. In comparison with these operations, HNL1 exhibits rock mass characteristics broadly comparable to Chuquicamata underground mine and stress magnitudes similar to those encountered in deep sectors of El Teniente (Cuello & Newcombe 2018). The combination of depth, stress and structural complexity places HNL1 at the upper bound of contemporary block cave design challenges.

* Corresponding author. Email address: Lawrence.Rwodzi@riotinto.com

Panel 0 (P0) represents the first mining block at HNL1 and was undercut and established between January 2022 and April 2024. As the inaugural panel, it provides the first opportunity to validate the geotechnical basis of design (BoD) against observed performance under full-scale operating conditions. The performance data obtained from P0 therefore represent a rare and valuable dataset for assessing block cave behaviour in deep, high-stress porphyry environments.

This paper documents the geotechnical BoD developed for HNL1 and assesses P0 cave and footprint performance relative to BoD predictions. The objective is to quantify how well key design assumptions aligned with observed behaviour and to extract geotechnical learnings applicable to future large, deep block caves developed in similarly challenging geological settings.

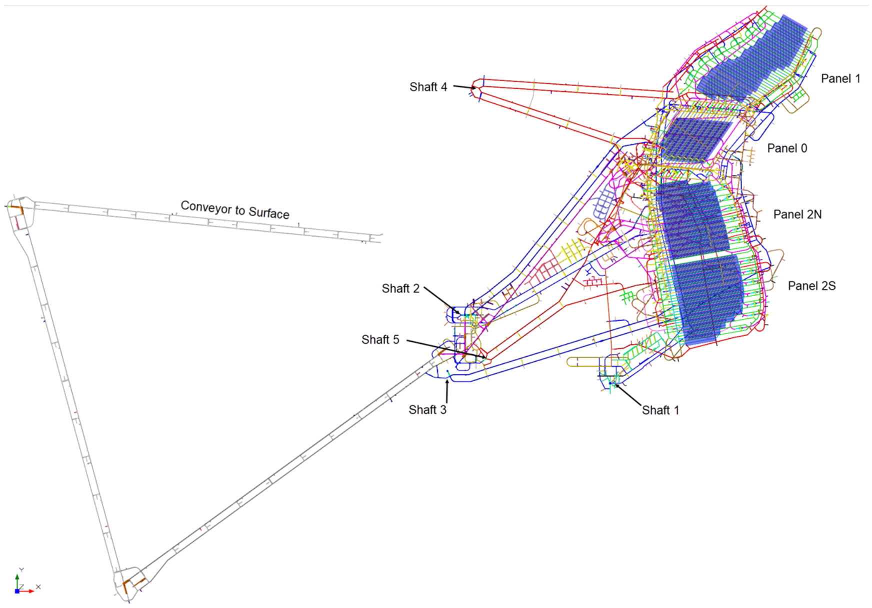

Figure 1 Hugo North Lift 1 mine layout

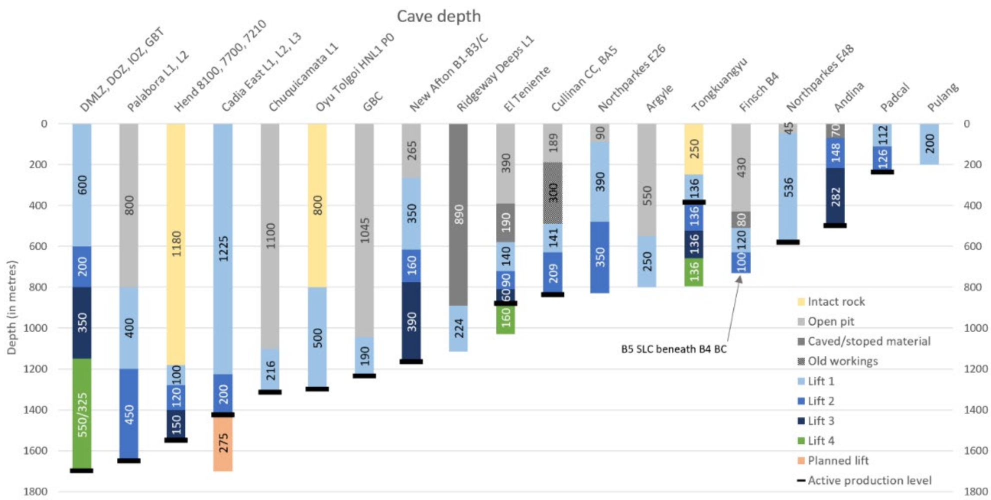

Figure 2 Benchmarking of the Hugo North Lift 1 block cave against industry caving operations (Mawdesley & Altankhuu 2026)

2 Geology and geotechnical environment

The geotechnical environment at HNL1 is governed by the interaction of three principal factors: pronounced structural complexity associated with multiple major fault systems, fair-to-poor rock mass quality and high in situ stress at extraction level depth. Together, these factors control excavation stability, cave initiation behaviour, and long-term infrastructure performance. In addition, the mineralised column extends up to approximately 400 m above the extraction level and is overlain by nearly 900 m of competent waste rock, requiring a design that balances effective stress management with reliable cave propagation.

2.1 Geology and structural complexity

The Hugo North deposit comprises porphyry-style copper–gold mineralisation associated with quartz monzodiorite intrusions emplaced beneath a deformed Upper Devonian to Lower Carboniferous sedimentary and volcanic sequence (Figure 3). The orebody is elongate, oriented approximately north-northeast to south-southwest and extends over more than 2 km in strike length (Figure 1).

The principal mineralised lithologies – Quartz Monzodiorite (QMD), Augite Basalt (VA) and Ignimbrite (IGN) – are cut and overlain by the late- to post-mineralisation intrusive phase biotite granodiorite, which forms a dyke system along the western and central portions of the deposit (Figure 3). These units are variably affected by porphyry-style alteration assemblages potassic, propylitic, advanced argillic and intermediate advanced argillic alteration.

The deposit is characterised by pronounced structural complexity resulting from multiple generations of faulting (Figure 3). Major fault zones define geotechnical domain boundaries, localise alteration and significantly degrade rock mass quality. These structures exert a strong control on excavation stability, undercut initiation behaviour and cave propagation.

The Lower Fault Zone is the most significant structural feature affecting HNL1, particularly P0. Its intersection with the original feasibility-stage extraction footprint posed unacceptable risks to drawpoint stability and materials handling infrastructure. Improved delineation of this structure through detailed face mapping and integration into the geotechnical model was therefore a primary driver for subsequent revisions to footprint geometry, infrastructure placement, undercut initiation strategy and macroblock sequencing adopted in the current design.

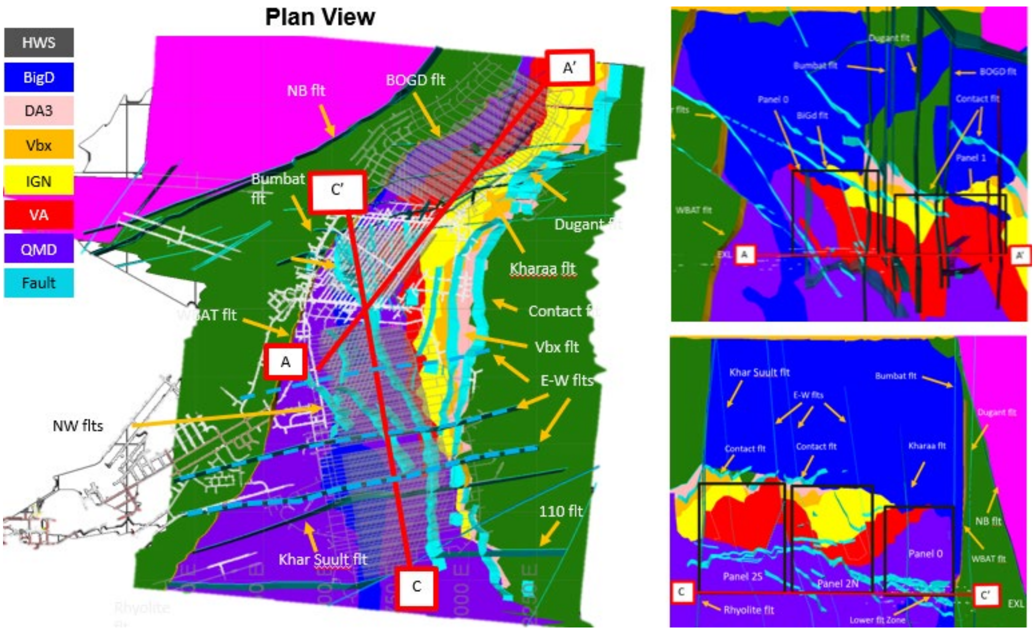

Figure 3 Hugo North Lift 1 lithology and major faults (extraction level plan and section views)

2.2 Rock mass characterisation

The HNL1 rock mass model was developed a comprehensive dataset consisting of approximately 130 km of drillcore logging, 4,300 face maps representing roughly 15 km of underground development and 2,712 uniaxial compressive strength (UCS) and triaxial compressive strength (TCS) intact strength tests (Rwodzi et al. 2026). From this dataset an integrated HNL1 3D geotechnical rock mass block model was developed using geostatistical estimation methods (Rwodzi et al. 2026). The rock mass model captures geotechnical domains defined based on lithology, alteration, weak veinlet density and structural boundaries (Figure 4a). The rock mass quality across HNL1 ranges from poor to fair, with typical RMR_{L90} (Laubscher 1990) between 40 and 55 within the orebody and values of 25–35 within major fault zones (Figure 4b). The global rock mass strength represents a highly variable moderate-to-weak rock mass (major fault zones ~2–3 MPa; footprint ranging from ~6–18 MPa), Figure 5.

The fair-to-poor rock mass quality, combined with high in situ stress, results in stress-to-strength ratios (σ_1/UCS) ranging from approximately 0.5 to 1.4 across the footprint, with the highest ratios occurring in weaker structural domains. These ratios strongly influenced the selection of advanced undercutting, drawpoint pillar enlargement and conservative infrastructure placement adopted in the BoD.

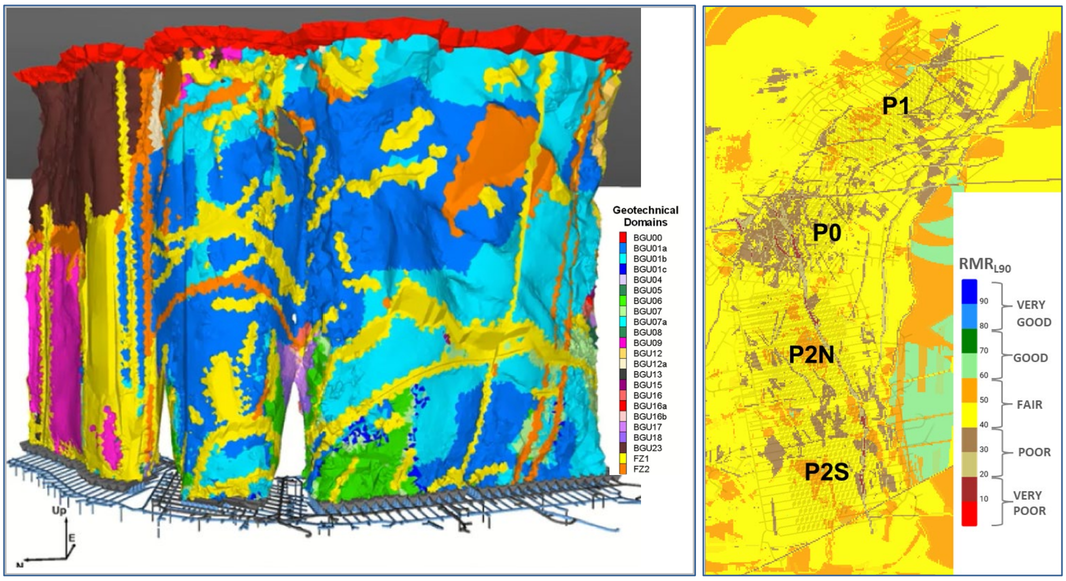

(a) (b)

Figure 4 Hugo North Lift 1 geotechnical domains. (a) Cave column; (b) Rock mass rating (footprint)

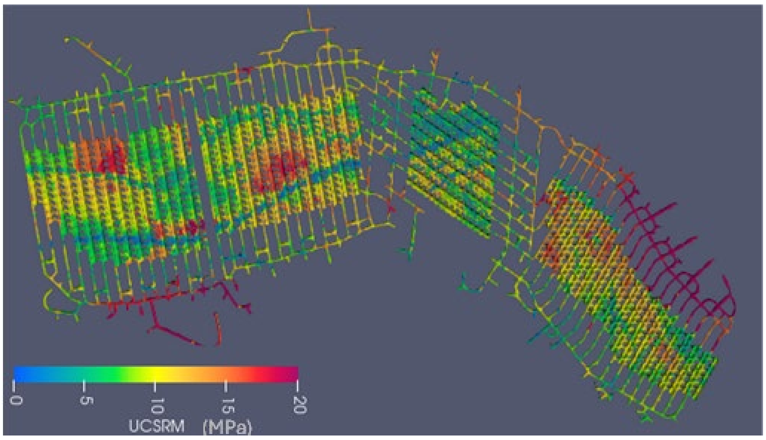

Figure 5 Hugo North Lift 1 global rock mass strength on extraction level

2.3 In situ stress regime

Three depth-dependent stress domains were defined based on over-coring stress measurements. At the HNL1 extraction level depth of approximately 1,300 m (Domain 3), the in-situ stress field is as follows:

- Major principal stress is sub-horizontal with a magnitude of approximately 57.8 MPa, oriented at an azimuth of 054°.
- Intermediate principal stress is sub-vertical at approximately 34.5 MPa.

- Minor principal stress is approximately 27.2 MPa, oriented at an azimuth of 144˚.

This stress regime produces elevated mining-induced stresses during undercutting and cave propagation, particularly in the abutment zones adjacent to the cave footprint. Effective management of these stresses was a key design driver, governing the selection of undercut methodology, undercutting direction, extraction level geometry, pillar sizing and macroblock sequencing.

3 Design evolution

The HNL1 mine design (Figure 6) evolved significantly from the original feasibility study to execution (Stegman et al. 2022). The evolution was driven by progressively improved geological and geotechnical knowledge derived from extensive face mapping during the development of Panel 0, resulting in refined structural and rock mass models, and updated numerical analyses supported by an expanding geotechnical database.

Updated numerical modelling identified several key risks in the feasibility-stage design, including potential orepass instability within faulted ground, severe stress concentrations affecting materials handling system (MHS) infrastructure within the cave initiation zone, factors of safety below unity for the original 28 × 15 m drawpoint pillars under peak abutment loading, excessive rim drive convergence with a 45 m offset from the extraction footprint, and cave initiation geometries that increased mining-induced stresses on subsequent adjacent panel development (Figure 6a).

In response, a series of targeted design modifications were evaluated using updated numerical models incorporating refined structural interpretations, revised rock mass properties, mining layout and sequences. Key changes included relocation of MHS infrastructure outside the extraction footprint, enlargement of drawpoint pillar dimensions to 31 × 18 m, extending rim drive offsets to 60 m, reorienting extraction and undercut drives relative to the principal stress direction, dominant structural sets, and practical operational considerations, and revising macroblock sequencing to better manage mining-induced stress during cave growth (Figure 6b).

The revised design reduced predicted excavation damage, convergence and stress concentrations, while improving drawpoint pillar stability and protecting critical infrastructure. This design formed the geotechnical basis of design (BoD) adopted for execution and the basis against which P0 performance was assessed.

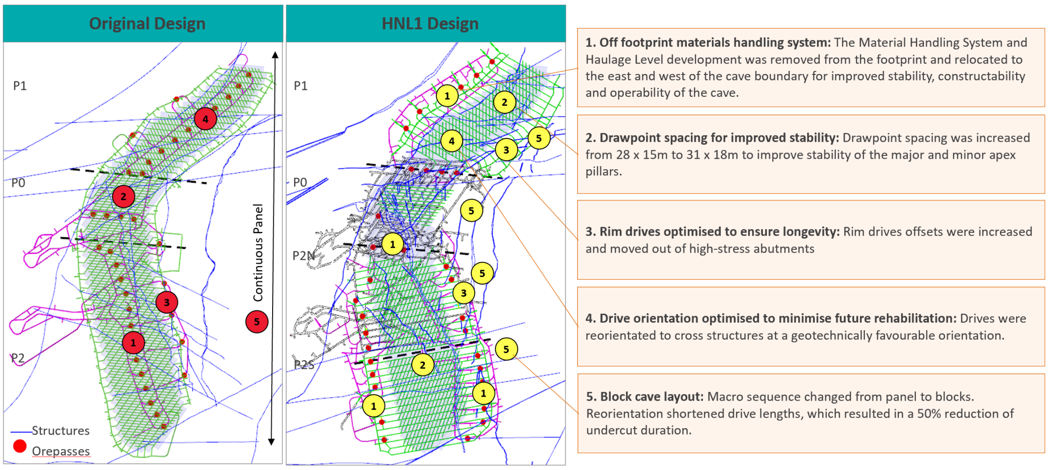

(a) (b)

Figure 6 Hugo North Lift 1 design evolution. (a) Original design; (b) Updated HNL1 design

4 Geotechnical basis of design

The geotechnical BoD for HNL1 was developed through a multicriteria optimisation process aimed at balancing caveability, stress management, infrastructure survivability and drawpoint productivity over the full life of each panel. Design decisions were informed by empirical caveability assessments, benchmarking against deep cave operations, and site-specific numerical modelling incorporating representative rock mass, structural, stress and production parameters.

4.1 Block size, caveability and interblock pillars

Larger cave footprints promote caveability and upward propagation through the high mineralised column; however, increasing block size also elevates abutment stresses at the extraction level and increases convergence in rim drives and drawpoints. Block size sensitivity studies demonstrated that blocks equivalent to approximately 8 to 11 extraction drives provided an acceptable balance between caveability and stress-related damage, maintaining predicted convergence and pillar factors of safety within design limits.

Between Panel 2N and 2S, inter-panel pillars were required to manage abutment stress and associated damage during block transitions and protect critical infrastructure during sequential mining. A 30 m inter-block pillar width (undercut-to-undercut) was selected following trade-off studies evaluating several options (Figure 7b). While wider pillars provided improvements in abutment stability (Figure 7a), they imposed unacceptable constraints on MHS layout and undercut sequencing and were therefore not adopted. Not leaving pillars between blocks was not technically viable (Figure 7c). The P0 pillars (96–125 m) were designed to ensure the long-term stability and serviceability of the P0 MHS now located within them.

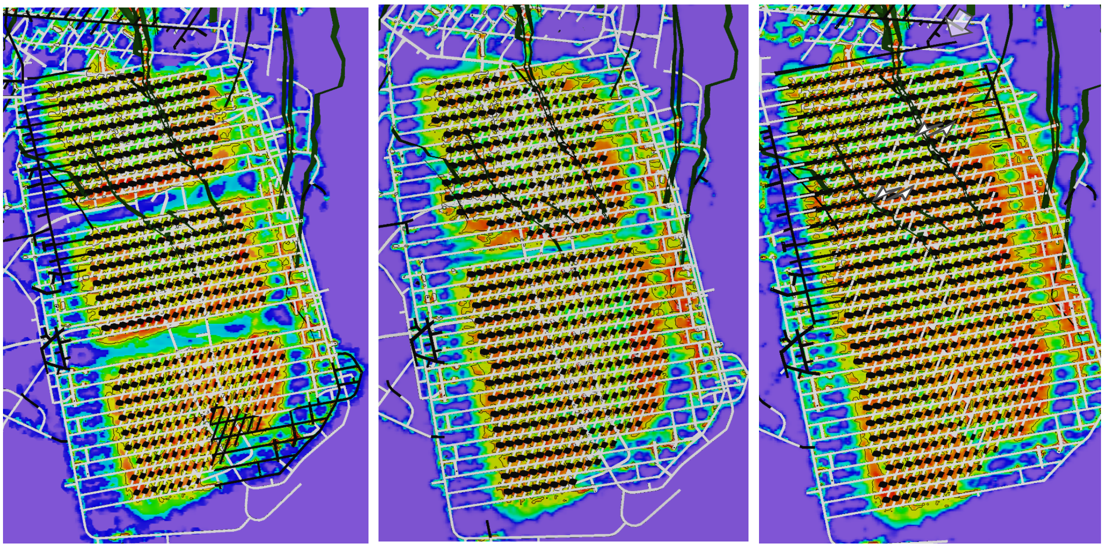

(a) (b) (c)

Figure 7 Block size geometry versus footprint stability. (a) Rock mass damage in 60 m inter-block pillars; (b) 30 m inter-block pillars; (c) No inter-block pillars

4.2 Caveability assessment

Preliminary caveability was initially assessed using the Laubscher caveability chart, incorporating high-stress adjustments across the range of anticipated Mining Rock Mass Ratings (MRMR). These assessments indicated a critical hydraulic radius (HR) between approximately 13–23 m for the Lift 1 blocks (Figure 8a). Given the depth, stress conditions and structural complexity of HNL1, empirical methods were treated as preliminary screening tools only (Brown 2007; Laubscher et al. 2017).

Final caveability assumptions were informed by coupled numerical modelling that explicitly represented the rock mass domains, major and minor structures, planned undercut strategy, undercutting advance direction and production schedules. The resulting HR for the blocks ranged from 18–23, corresponding to 16–24 drawbells fired, based on bell firing sequence. For the P0 block, the modelling predicted a critical HR was approximately 23 m (Figure 8b), corresponding to sustained cave propagation following approximately 21 drawbells. These predictions formed the basis for cave initiation planning and drawbell firing rules.

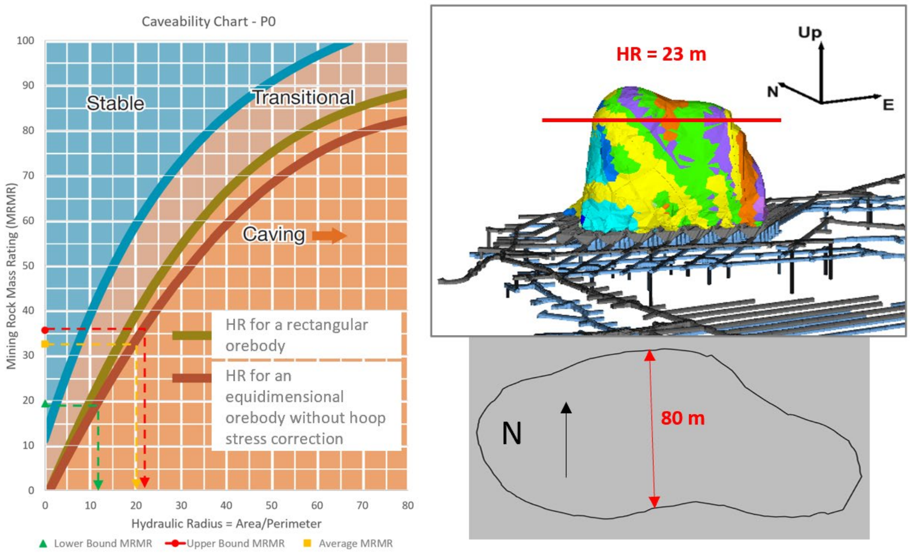

(a) (b)

Figure 8 (a) Hydraulic radius (HR) on Laubscher's empirical chart; (b) Couple modelling

4.3 Drive orientation, undercut face orientation and block sequence

Extraction and undercut production drives varied between the mining blocks, representing a compromise between drive alignment to stress, structure, undercutting face direction, undercutting duration and mine layout constraints imposed by footprint geometry and materials handling requirements. The associated reduction in drive stability relative to an optimal stress-parallel orientation was quantified through pillar stability analyses and assessed as acceptable given the installed support systems.

Block sequencing balanced the management of the high mining-induced stresses associated with the adjacent active mining block while accommodating the geotechnical and operational constraints influencing drive orientation. The sequence was designed to eliminate primary-secondary block interactions, promote cave growth from a developing cave to an established cave, and manage stress levels in the undercut and material handling system infrastructure as the caving footprint expanded. P0 is the first mining block in the sequence, followed by Panel 2 North (P2N), Panel 2 South (P2S) and Panel 1 (P1). Geotechnically, the commencement of the P1 undercut is only constrained by the completion of P0 undercut.

Figure 9 provides the final drive layout, undercutting direction and block sequencing. As P0 was already in development, the adoption of P0 BoD informed subsequent panel design. Undercut face orientations were selected to avoid breasting major structures and to maintain undercut backs in comparatively lower-stress configurations, consistent with established industry practice (Brown 2007; Laubscher et al. 2017).

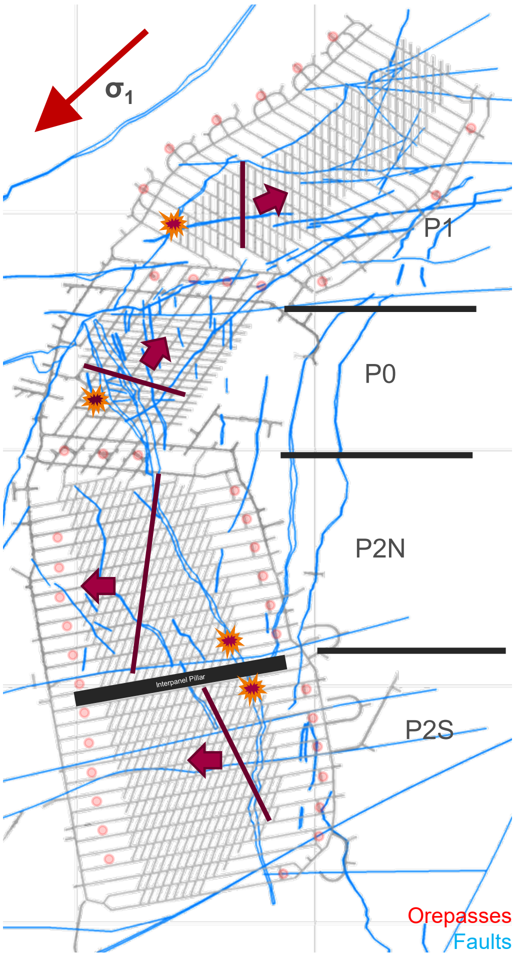

Figure 9 Hugo North Lift 1 macroblock sequencing

4.4 Undercutting methodology

The advanced undercut methodology (Butcher 1999; Butcher 2000; Trueman et al. 2002; Laubscher et al. 2017) was selected to manage the high mining-induced stresses anticipated at extraction level depth in moderate-strength rock mass conditions. In this approach, the undercut horizon advances ahead of extraction level development, establishing a destressed shadow zone in which drawpoint drives and drawbell infrastructure are constructed.

A straight-front undercut configuration was adopted with a target advance rate of 2,700 m²/month and dynamic lead–lag tolerances of ±10 m. This configuration provided operational flexibility while maintaining effective stress shielding for drawpoint drive development (Figure 10). The stress shielding angles were varied according to the stage of undercutting and cave initiation.

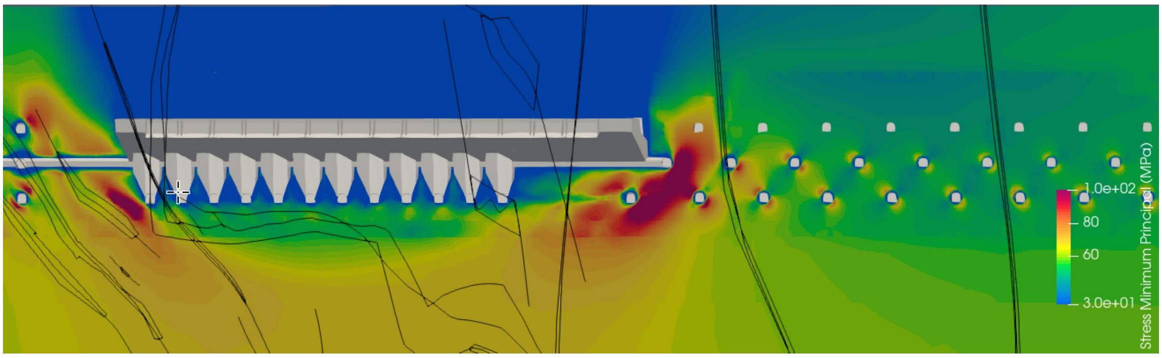

Figure 10 Advanced undercut stress shielding

4.5 Undercut initiation

Mining-induced stress analyses indicate that development of the P0 block cave generates elevated stress concentrations in the northwest and southeast corners of the footprint (Figure 11). As a result, the northeastern region of P2N is located within an elevated stress field influenced by prior cave development. Selection of undercut initiation locations and directions therefore required careful consideration of the evolving mining-induced stress environment, balanced against operational constraints associated with the MHS layout and undercut construction logistics.

Primary geotechnical considerations for undercut initiation included mining away from, or parallel to, adjacent active or future mining blocks, and avoiding undercut advance directly toward neighbouring cave footprints. This approach was adopted to limit the accumulation of unfavourable abutment stresses at the undercut front and to reduce stress interaction between adjacent panels during early cave growth.

Ground conditions also influenced initiation strategy. Where poor-quality ground presented a dominant stability risk, the preferred approach was to initiate the cave within weaker rock and advance toward stronger ground, thereby progressively improving excavation stability. In some cases, this preference was moderated by caveability considerations, where initiating undercutting within stronger rock was advantageous for establishing reliable cave propagation. Final initiation strategies therefore reflected a balanced assessment of stress management, ground control risk, caveability and operational practicality.

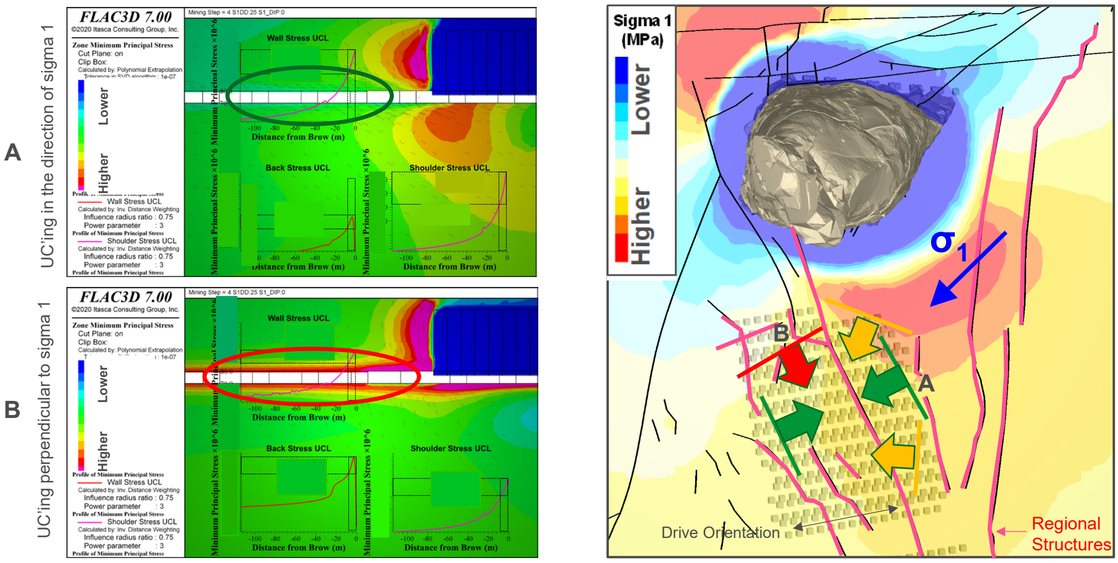

Figure 11 Undercutting direction relative to sigma 1 tradeoff

4.6 Rim drives, pillars and infrastructure protection

Rim drive offsets were increased from 45 m in the feasibility design to 60 m, placing drives within modelled lower rock mass damage zones beyond the peak abutment stress environment (Figure 12). Numerical modelling demonstrated that this offset significantly reduced convergence and rock mass damage potential without imposing excessive development requirements.

Drawpoint pillar geometry was increased from 28 × 15 m to 31 × 18 m following pillar stability analyses under peak loading conditions. In the redesign, precedence was given to footprint stability to enhance drawpoint longevity. Pillar orientation relative to σ_1 was explicitly considered to take advantage of orientation-dependent stress-strength behaviour. Industry benchmarking and both local- and mine-scale numerical modelling confirmed the revised geometry provided acceptable factors of safety throughout the panel life cycle.

Critical MHS infrastructure was relocated off the extraction footprint for all panels. This configuration removed ore passes and tipple points from the high-stress abutment environment, greatly reducing the risk of stress-induced damage and improving long-term serviceability.

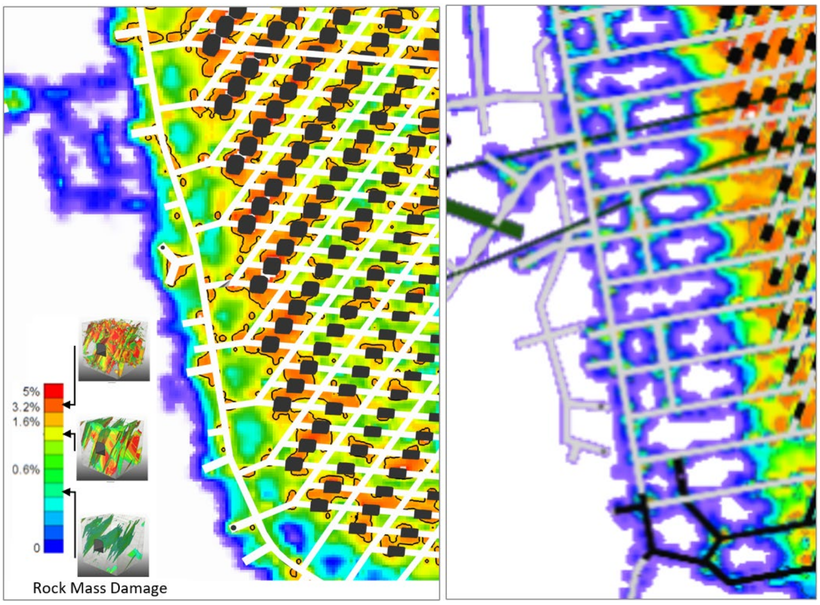

Figure 12 Modelled rock mass damage at 45 m (a) versus 60 m (b) rim drive offset

4.7 De-stress shadow and cave establishment rules

Cave establishment was governed by an HR adaptive protocol which links drawbell firing proximity to the maturity of the undercut and cave (Laubscher et al. 2017). Allowable drawbell firing positions and drawpoint drive turnout distances from the undercut front increased progressively with cave size as quantified by the HR, reflecting the evolving stress arch as the cave develops. This adaptive approach provides a controlled and defendable framework for managing stress during cave initiation and early cave growth while maintaining operational flexibility.

During early cave establishment (HR < 50%), undercut-induced stresses dominate and remain broadly comparable to in situ stress conditions. Under these conditions drawpoint drives can be pre-developed and drawbell firing is permissible in close proximity to the undercut front. Threshold distances of up to approximately 17 m behind the undercut front were adopted, subject to confirmation through rock mass response monitoring, with cave maturity measured by the number of bells fired.

During the intermediate stage of cave development (HR 50–100%), the cave footprint increases and stresses become increasingly influenced by both undercutting and cave-induced loading. In this stage, drawpoint drive development is restricted to approximately 17 m behind the undercut front, while drawbell firing is constrained to distances not less than 31 m from the undercut front, reflecting the growing influence of the developing stress arch.

Once the cave exceeds 100% of the design HR (HR > 100%), the cave propagates under its own geometry and mass, and cave-induced stresses dominate, extending further below the undercut level. Under these conditions, drawpoint drive development is limited to distances not less than 31 m, and drawbell firing is constrained to a minimum distance of 70 m from the undercut front to maintain stability within the extraction level.

In all stages, drawbell firing controls the rate of undercut advance, rather than the undercut dictating firing positions. The adopted threshold distances of 17, 31 and 70 m for HR < 50%, HR 50–100% and HR > 100%, respectively, were derived from site-specific numerical stress analyses.

4.8 Summary of basis of design parameters

A summary of the key geotechnical BoD parameters for each HNL1 panel is provided in Table 1.

Table 1 Summary of Hugo North Lift 1 geotechnical basis of design parameters across all panels

Parameter	P0	P1	P2N	P2S
Material Handling System location	Off footprint (north and south pillars)	Off footprint (west MHS)	Off footprint (east and west)	Off footprint (east and west)
Rim drive offset	45–60 m	60 m	60 m	60 m
Extraction Level Layout	El Teniente Layout			
Drawpoint pillar size	31 × 18 m (increased from 28 × 15 m)			
Inter-panel pillar	96–125 m, P0 to P1	96–125 m, P0 to P1	96–125 m, P0 to P2N	30 m, P2N to P2S
Footprint size	~320 × 280 m	~250 × 650 m	~340 × 430 m	~370 × 465 m
Level spacing (extraction to undercut; undercut to apex level)	17 m; 22 m	17 m; 22 m	17 m; 22 m	17 m; 22 m
Footprint production drive orientation to σ_1	~20°	~65°	~25°	~25°
Undercut face orientation to σ_1	~60°	~55°	~48°	~83°
Undercut initiation and direction	Southwest Initiation, UC direction from south to north	Southwest Initiation, UC direction from Southwest to northeast	Southeast initiation, UC direction from east to west	Northeast initiation, UC direction from east to west
Extraction Level veranda /de-stress shadow	60 m/17 m	70–90 m/40 m	70–90 m/40 m	80–100 m/40 m
Undercut lead/lag	±10 m dynamic	±10 m dynamic	±10 m dynamic	±10 m dynamic
Undercut type, shape,	Advanced, Straight	Advanced, straight	Advanced, straight	Advanced, straight
Undercut face length and rate	320 m, 2,700 m^2/month	260–430m, 2,700 m^2/month	420–455 m, 2,700 m^2/month	360–488 m, 2,700 m^2/month
Planned undercut duration	3 years	4.5 years	5 years	5 years

5 Panel 0 cave performance

Undercutting of P0 commenced in January 2022 and was completed in April 2024. Since first production, approximately 18 Mt has been mined, and production has ramped up to the nominal nameplate rate of approximately 30 ktpd. The cave has successfully propagated to surface and the panel is operating in full production with approximately 95% drawpoint availability, demonstrating excellent footprint serviceability.

Overall, P0 performance has closely matched the predictions and acceptance criteria defined in the BoD. Rock mass conditions encountered during development and undercutting aligned well with the pre-mining geotechnical block model, with no material changes required to domain definitions or rock mass property assumptions. Continuous calibration through face mapping has primarily improved fault characterisation rather than altering baseline geotechnical assumptions.

The advanced undercut achieved sustained advance rates of approximately 3,000–3,500 m²/month, exceeding the design target of 2,700 m²/month. The undercut was completed in approximately 28 months, significantly ahead of the planned three-year schedule, with no delays attributable to geotechnical instability. Operational optimisation to a smaller W undercut shape and good blasting practice contributed to this success. Caving initiated at an HR consistent with the predicted critical value of approximately 23 m, as confirmed by cave monitoring instrumentation.

Extraction level infrastructure has performed within design expectations to date, with no major rehabilitation required during undercutting to date. As shown in Figure 13, mapped damage levels in extraction level drives and rim drives show predominantly minor to moderate damage and remains within acceptable serviceable limits. Measured convergence has generally been in the order of 100–200 mm. Rim drives, at the 60 m offset, remain fully accessible and serviceable, confirming the effectiveness of the revised setback adopted in the BoD. Localised severe to very severe damage (Figure 13) observed at selected tipple points, rim drives and isolated areas of the footprint has been structurally controlled and successfully managed through targeted support and monitoring. Overall, observed infrastructure performance supports the conclusion that the original design configuration would likely have resulted in significantly higher damage levels and reduced long-term serviceability, especially in fault zones and high stress areas.

The HR-adaptive drawbell firing protocol and associated de-stress shadow criteria were implemented with a high level of compliance. Drawbell breakaways and construction were successfully completed within the designed destressed zone, supporting safe and efficient cave establishment. Successful cave break through to surface eliminated airblast risk and avoided the ramp-up delays commonly associated with cave stalls.

Observed subsidence development and fracture zone extent are broadly consistent with numerical predictions and are strongly influenced by geological structures. Ongoing analysis of cave propagation, subsidence monitoring and deformation data will further refine the quantitative validation of BoD assumptions as mining progresses.

Collectively, the observed cave response, infrastructure performance and production outcomes demonstrate that the key geotechnical assumptions and design criteria adopted in the BoD have been validated through operating experience. Table 2 provides a summary of key performance milestones.

Table 2 Panel 0 performance key milestones

Basis of design element	Basis of design prediction	Observed performance
Rock mass model	RMR_{L90} 40–55 (P50) across footprint, 25–35 within major fault zones.	Continuous rock mass calibration resulted in minimal change to rock mass property assumptions. Improvements made in fault characterisation (Rwodzi et al. 2026)
Extraction level Footprint availability (drawpoints pillars)	Number of available drawpoints Factor of Safety > 1.5;	95% drawpoint availability. No major rehab triggered during undercutting, convergence within 100–200 mm to date. Minor to Moderate Damage observed through most of footprint (Figure 13). Localised severe damage through major fault areas
Rim drive stability	Serviceable at 60m Offset	100% rim drive availability. Cumulative damage mapping (Figure 13) shows minor to moderate damage, localised severe damage triggering TARP Level 3
Advance undercut advance rate	2,700 m²/month; 3-year duration. 10 m /month Straight shape Big W shaped UC	3,000 to 3,500 m²/month achieved in 28 months. Straight advance undercut. UC shape modified to small W shape, contributing to faster UC rates. 100% drill drive availability during undercutting
Caving initiation hydraulic radius	100% Hydraulic Radius = 23 m (21 drawbells)	100% HR confirmed at 23 m, 21 drawbells. HR confirmed using cave monitoring instrumentation (Bayar et al. 2024)
Material handling system	Serviceable through life of Block	100% availability of MHS tipples and ore passes to date Manageable convergence observed at tipples 1 and 4 (Figure 13)
Cave breakthrough/subsidence	Successful cave propagation and breakthrough with no stall. Propagation and subsidence fracture zones are structurally controlled.	No cave stall. Surface breakthrough achieved eliminating airblast risk. Propagation and fracture zones are structurally controlled.

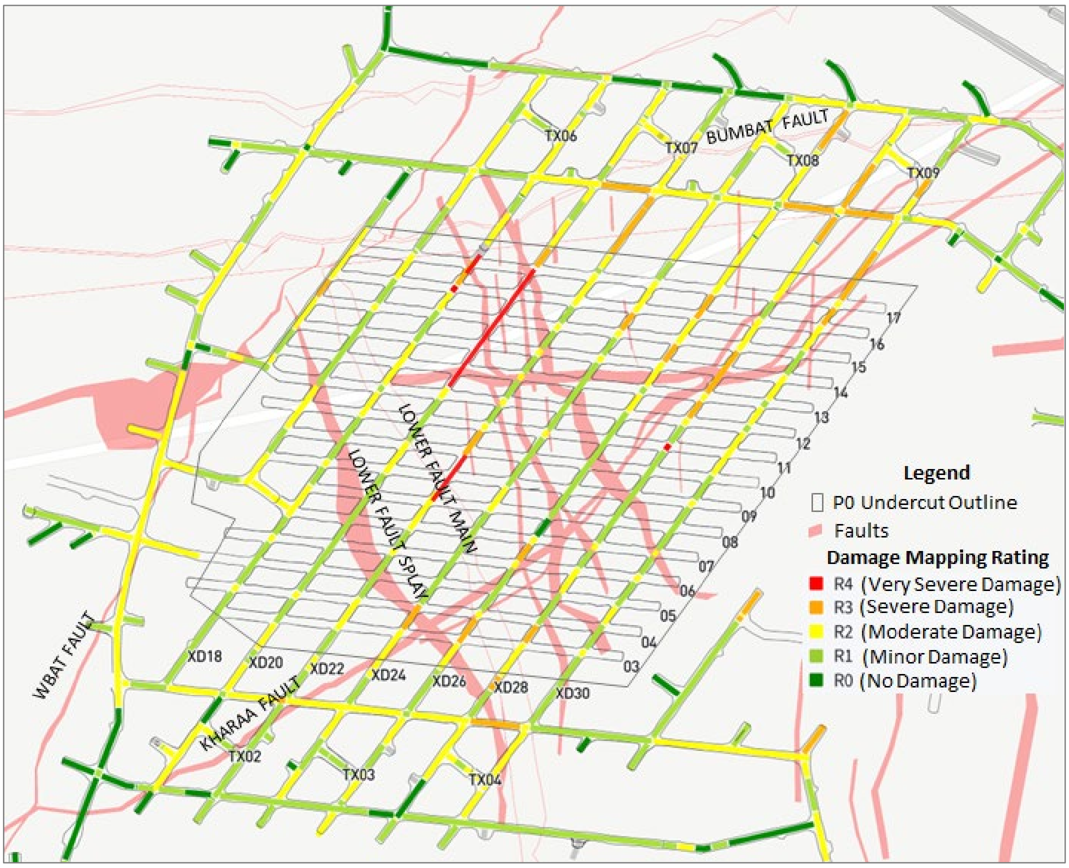

Figure 13 HNL1 P0 extraction level damage mapping

6 Conclusion

This paper has presented the geotechnical BoD for the Hugo North Lift 1 (HNL1) block cave at Oyu Tolgoi and assessed the early cave performance from the Panel 0 (P0) development and undercutting campaign completed between 2022 and 2024. HNL1 represents one of the world's deepest commissioned block caves in a porphyry setting and operates under a combination of depth (~1,300 m), high in situ stress ($\sigma_1 \approx 57.8$ MPa) and poor-to-fair rock mass conditions for which published performance data are limited.

The BoD reflects more than a decade of iterative geotechnical learning, underpinned by progressively refined geological and rock mass models, stress measurements and large-scale numerical analyses. Five targeted design modifications – most notably the adoption of advanced undercutting, increased drawpoint pillar dimensions, increased rim drive offsets, off-footprint placement of materials handling infrastructure, and revised macroblock sequencing – were introduced to address the combined challenges of high stress, structural complexity and infrastructure survivability.

Early cave performance of P0 demonstrates strong alignment with BoD predictions. The advanced undercut was completed ahead of schedule, achieving sustained advance rates of 3,000–3,500 m²/month against a planned rate of 2,700 m²/month, with no undercut-related production delays. Cave initiation occurred at an observed hydraulic radius (HR) consistent with the predicted critical value of 23 m, and continuous cave propagation to surface was achieved without stalling. The enlarged 31 × 18 m drawpoint pillar geometry, 60 m rim drive offset, HR-adaptive drawbell firing rules and off-footprint materials handling system configuration have all met or exceeded performance criteria to date, with convergence and damage remaining within design thresholds across the extraction level.

The successful breakthrough to surface is a particularly significant outcome as it eliminated airblast risk and enabled uninterrupted ramp-up to nameplate production. Observed cave propagation behaviour and subsidence response are largely consistent with modelling predictions and are strongly influenced by geological structures, reinforcing the importance of structural representation in deep cave design.

These outcomes reflect not only the robustness of the basis of design, but also the disciplined execution and operational optimisation through which it was delivered. P0 at HNL1, therefore, provides a rare, validated geotechnical reference case for deep, high-stress porphyry block caving under fair-to-poor rock mass conditions. Ongoing back-analysis of cave growth rates, subsidence extent and monitoring data will further strengthen the quantitative validation of the BoD assumptions. Future publications will integrate performance data from subsequent panels, extending the dataset and contributing to improved confidence in the design and execution of large, deep block caves developed in similarly challenging geotechnical environments.

Acknowledgement

The authors would like to acknowledge the contributions of the OT technical and strategic mine planning team for work contributing to the HNL1 design, and OT site geotechnical and operational teams for the development and successful execution of HNL1. The authors gratefully acknowledge Oyu Tolgoi LLC and Rio Tinto for granting permission to publish this work.

Please note that this paper contains estimates, projections, and forward-looking statements within the meaning of applicable securities laws. These statements are based on operational observations, historical performance data, engineering studies, modelling assumptions, current operating conditions and interpretations available at the time of writing. Actual outcomes may differ due to operational, geotechnical, regulatory, market and other factors.

References

Bayar, E, Simanjuntak, K, Birch, D, Mardiansyah, F & Purwanto, H 2024, ‘Seismological data and analysis for the early stages of block caving’, in D Johansson & H Schunnesson (eds), *MassMin 2024: Proceedings of the International Conference & Exhibition on Mass Mining*, Luleå University of Technology, Luleå, pp. 893–908, https://doi.org/10.36487/ACG_repo/2435_G-02

Brown, ET 2007, *Block Caving Geomechanics*, Julius Kruttschnitt Mineral Research Centre, University of Queensland, Brisbane.

Butcher, RJ 1999, ‘Design rules for avoiding draw horizon damage in deep level block caves’, *Journal of the Southern African Institute of Mining and Metallurgy*, vol. 99, no. 3, pp. 151–155.

Butcher, RJ 2000, ‘Block cave undercutting – aims, strategies, methods and management’, in G Chitombo (ed.), *Proceedings of MassMin 2000*, Australasian Institute of Mining and Metallurgy, Melbourne, pp. 405–411.

Cuello, D & Newcombe, G 2018, ‘Key geotechnical knowledge and practical mine planning guidelines in deep, high-stress, hard rock conditions for block and panel cave mining’, in Y Potvin & J Jakubec (eds), *Caving 2018: Proceedings of the Fourth International Symposium on Block and Sublevel Caving*, Australian Centre for Geomechanics, Perth, pp. 17–36, https://doi.org/10.36487/ACG_rep/1815_0.2_Cuello

Mawdesley, C & Altankhuu, B 2026, 'Global benchmarking of block caves – a super cave update', in A van As, D Cumming-Potvin & J Wesseloo (eds), *Caving 2026: Proceedings of the Sixth International Conference on Block and Sublevel Caving*, Australian Centre for Geomechanics, Perth, https://doi.org/10.36487/ACG_repo/2645_03

Laubscher, DH 1990, ‘A geomechanics classification system for the rating of rock mass in mine design’, Journal of the South African Institute of Mining and Metallurgy, vol. 90, no. 10, pp. 257–273.

Laubscher, DH, Guest, AR & Jakubec, J 2017, *Guidelines on Caving Mining Methods: The Underlying Concepts,* W.H. Bryan Mining and Geology Research Centre, Sustainable Minerals Institute, The University of Queensland, Brisbane.

Rwodzi, L, Ekkerd, J, Taylor, T, Batsaikhan, A, Russo, A, Ramirez, C, Hormazabal, E, Nur, J, 2026, ‘Geotechnical characterisation of Hugo North Lift 1, Oyu Tolgoi’, in A van As, D Cumming-Potvin & J Wesseloo (eds), *Caving 2026: Proceedings of the Sixth International Conference on Block and Sublevel Caving*, Australian Centre for Geomechanics, Perth, https://doi.org/10.36487/ACG_repo/2645_73

Stegman, CL, Togtokhbayar, O, Herselman, S & Altankhuu, B 2022, 'Oyu Tolgoi: engineering a Mongolian caving dynasty', in Y Potvin (ed.), *Caving 2022: Proceedings of the Fifth International Conference on Block and Sublevel Caving*, Australian Centre for Geomechanics, Perth, pp. 625-634

Trueman, R, Pierce, M & Wattimena, R 2002, ‘Quantifying stresses and support requirements in the undercut and production level drifts of block and panel caving mines’, *International Journal of Rock Mechanics and Mining Sciences*, vol. 39, no. 5, pp. 617–632.